Electronic Supplementary Material (ESI) for Journal of Materials Chemistry C.

Electronic Supplementary Information

$Sn(SCN)_2$ as an Additive for Improving Hole Transport Properties of PEDOT:PSS in Organic Photovoltaics

Jidapa Chaopaknam,[ab] Taweesak Sudyoadsuk,[a] Vinich Promarak,[a] Akinori Saeki,[b] and Pichaya Pattanasattayavong*[a]

[a] Department of Materials Science and Engineering, School of Molecular Science and Engineering, Vidyasirimedhi Institute of Science and Technology (VISTEC), Rayong 21210, Thailand

[b] Department of Applied Chemistry, Graduate School of Engineering, Osaka University, 2-1 Yamadaoka, Suita, Osaka 565-0871, Japan

* Corresponding author. Email: pichaya.p@vistec.ac.th

Experimental

$Sn(SCN)_2$ Solution Preparation. Tin (II) thiocyanate [$Sn(SCN)_2$] was synthesized following the reported procedure.[1] The acquired $Sn(SCN)_2$ crystals were then ground under 40% RH (relative humidity) to decrease the particle size and improve the dissolution. The $Sn(SCN)_2$ solution was prepared using 1-propanol (> 99.5%, TCI) at various concentrations of 10, 20, 30 and 40 mg mL^{-1}. The solution was stirred for 2 h and filtered by a polytetrafluoroethylene (PTFE) filter with 0.22-μm pore size under inert N_2 atmosphere inside a glove box prior to usage.

PEDOT:PSS Film Fabrication. Substrates were cleaned by 1% v/v detergent solution (Liquinox, Alconox Inc.), deionized water, acetone, and isopropanol. For each step, the substrates were placed in an ultrasonication bath for 20 min. Next, the substrates were dried with a N_2 stream and treated with UV-ozone for 15-20 min. To prepare the PEDOT:PSS-$Sn(SCN)_2$ samples, $Sn(SCN)_2$ solutions of varying concentrations (from the previous step) were added with a constant volume of 20 μL into 380 μL of the parent PEDOT:PSS solution (Clevios AI 4083, Heraeus), yielding $Sn(SCN)_2$ concentrations of 0.05, 0.10, 0.15, and 0.20% w/v. The solutions were then blended by stirring for 30 min and filtered by a polyvinylidene fluoride (PVDF) filter with 0.45-μm pore size. The pH of the solutions was measured with a Horiba LAQUAtwin pH meter. The prepared solutions were spin-coated onto the cleaned substrates at 5000 rpm for 30 s, and the films were annealed at 150 °C for 10 min under ambient conditions. For solar cell fabrication, the prepared films were transferred to a glove box.

Drop-cast Sample Preparation. To improve the signal intensity for Raman spectroscopy, samples were prepared by drop-casting. The pristine and $Sn(SCN)_2$-added PEDOT:PSS solutions were drop-

cast onto substrates pre-heated to 120 °C and left for 10 min to completely evaporate the solvent. This process was carried out under ambient environment.

Raman Spectroscopy. Drop-cast samples were analyzed using a Bruker Senterra dispersive Raman microscope. The measurements were performed with a 532-nm laser excitation operated at 2 mW. All Raman spectra were obtained by a 10x objective lens and 20-s acquisition time. Data analysis was conducted using OPUS software.

X-ray Photoelectron Spectroscopy (XPS). The chemical analysis of thin films was carried out by using a Jeol JPS9010MC photoelectron spectrometer equipped with a monochromator. The X-ray source was Al K_α operated at a 24-kV bias. XPS spectra were recorded with a pass energy of 50 eV for survey scans and 10 eV for core-level scans under a base pressure of 10^{-7} Pa. Charge neutralization was required for the measurements by using an electron flood gun with an acceleration voltage of 2 V and an emission current of 5 mA. The data was averaged from 75 scans and analyzed by SpecSurf software. Binding energies of the samples were aligned to the adventitious carbon position (C 1s at 284.8 eV).

UV-Visible-Near Infrared Spectroscopy (UV-Vis-NIR). Thin-film samples were deposited on quartz substrates following the procedure described above. Optical transmission and reflection spectra were measured in a wavelength range of 200 – 2000 nm using a PerkinElmer LAMBDA 1050 spectrophotometer equipped with an integrating sphere. The absorption spectra were calculated using the Beer-Lambert law, and the optical band gap values were determined using Tauc plots.

Photoelectron Yield Spectroscopy (PYS). The ionization potentials were characterized using a BUNKOUKEIKI BIP-KV216K instrument. All samples were prepared on indium tin oxide (ITO) substrates by spin-coating following the abovementioned procedure. The photoelectron yield was recorded as a function of the excitation energy which was generated by a deuterium lamp (30 W) with an energy range of 4.0 – 9.5 eV. All measurement was operated under vacuum condition at 5×10^{-3} Pa. The ionization potentials which are related to the valence band maxima (VBM) or the highest occupied molecular orbital (HOMO) energy levels were determined from the threshold energies of the yield$^{1/2}$ spectra.

Kelvin Probe (KP) Measurements. Work functions or Fermi energy levels (E_F) of film samples deposited on ITO substrates were measured using a KP Technology KP020 system. The data were calculated from the contact potential difference between the analyzed films and an Au reference of a known work function, obtained separately from a PYS measurement. All measurements were performed under ambient condition.

X-ray Diffraction (XRD). The structural analysis was performed using a Bruker D8 Advance diffractometer in powder mode (PXRD). The measurements were operated using a Cu K_α X-ray source (λ = 1.5406 Å). The diffraction patterns were recorded over a 2θ range between 2° and 40° with a measurement step of 0.05°.

Time-Resolved Microwave Conductivity (TRMC). Pristine and $Sn(SCN)_2$-treated PEDOT:PSS films were prepared on quartz substrates with dimensions of 24×11 mm^2 by spin-coating. The measurement

area of 11×11 mm^2 was defined by an adhesive tape. The TRMC setup was a custom-made system at Osaka University. The samples were packed in a sealed chamber under N_2 atmosphere and set in a resonance cavity. Charge carriers were generated by the second harmonic generation (SHG, λ = 532 nm), seeded by a Spectra-Physics Quanta-Ray Nd:YAG laser (ca. 9-ns pulse duration, 10 Hz), and probed by a continuous microwave with a frequency of 9.1 GHz. Specifically, a 5-mm spot of excitation source was fixed at 2 mW, achieving an incident photon density I_0 = 1.36×10^{15} photons cm^{-2} $pulse^{-1}$. The transient photoconductivity ($\Delta\sigma_{TRMC}$) was converted to the TRMC figure-of-merit, i.e., the product of the charge carrier generation quantum efficiency at the pulse end (ϕ) and the sum of charge carrier mobilities ($\Sigma\mu = \mu_h + \mu_e$), based on the following[4]

$$\phi\Sigma\mu = [\Delta\sigma_{\mathrm{TRMC}}/(qI_0\,F_{\mathrm{light}})] \tag{S1}$$

where q and F_{light} are the elementary charge and a correction (or filling) factor, respectively.

Four-Point Probe Measurements. The sheet resistance of samples was measured using a Jandel RM3000+ four-point probe. All samples were spin-coated on glass substrates. The data were recorded with an applied current of 10 nA. The resistivity (ρ) values of the film samples were calculated following[2]

$$\rho = \frac{RA}{L} \tag{S2}$$

in which R = electrical resistance, A = area, and L = length. Subsequently, the conductivity (σ) was calculated from the inverse of ρ.

Atomic Force Microscope (AFM). Thin-film morphology was studied using a Park System NX10 atomic force microscope with non-contact mode. The measurements were operated using Olympus OMCL-AC160TS cantilevers (n-Si, 7-nm tip radius, 300-kHz resonance frequency, 26-N m^{-1} spring constant). Root-mean-square roughness values (σ_{rms}) of the samples were obtained from 20x20 μm^2 images. All AFM images were processed in Gwyddion software.[3]

Profilometry. Film thicknesses were measured by a Bruker Dektak XT profilometer. For each sample, several scans were recorded, and the reported thickness is the average value.

Solar Cell Device Fabrication. Solar cells were fabricated on ITO-coated glass substrates (sheet resistance $\leq$ 20 Ω sq^{-1}, Instrument Glasses). The hole transport layers (HTLs) were pristine PEDOT:PSS or $Sn(SCN)_2$-treated PEDOT:PSS films prepared by spin-coating using the procedure described above. The bulk-heterojunction (BHJ) layer was prepared by first dissolving PTB7-Th (PCE10, Ossila) in chlorobenzene (anhydrous, 99.8%, Sigma-Aldrich) at a concentration of 8.8 mg mL^{-1} and stirring for 2 h. Next, the solution was filtered with a 0.22-μm PTFE filter, and 900 μL of the PTB7-Th solution was then pipetted to dissolve 13.2 mg of $PC_{71}BM$ (> 99%, Ossila), resulting in a blend solution in chlorobenzene. The BHJ solution was stirred at 75 °C for 8 h, and then 30 μL (3% v/v) of 1,8 diiodooctane (98%, TCI) was added. Subsequently, the active layer was spin-coated on the HTL at 1750 rpm for 30 s and treated with methanol (anhydrous, 99.8%, Sigma-Aldrich) as an antisolvent at 4000 rpm for 30 s. All fabrication processes of solar cells were done under inert atmosphere inside a glove box. The films were stored in a high-vacuum chamber (< 5×10^{-6} Torr) overnight prior to the next step. Finally, the solar cells with an active area of 0.0707 cm^2 were completed by thermally evaporating

10-nm bathocuproine (BCP, >99.0%, TCI) and 100-nm Al top contact through a shadow mask using an ALS Technology E200 physical vapor deposition system.

Solar Cell Characterization. Current density-voltage (*J*-*V*) characteristics of solar cells were measured with a source-measure unit (ADCMT 6241A) and a solar simulator (SAN-EI ELECTRIC XES-301S with AM1.5G filter) calibrated to 1 sun intensity with a photodiode reference device (S1137-1010BQ, Bunkoukeiki). All solar cell devices were enclosed in a sealed chamber to prevent the degradation during the measurement.

External Quantum Efficiency (EQE). EQE spectra were recorded by a BUNKOUKEIKI SM-250 measurement system. All samples were sealed in the closed chamber during this measurement. The monochromatic light was generated from a xenon lamp, and the spectra were measured in a wavelength range of 300 to 900 nm with a step of 5 nm. The intensity of irradiation at each wavelength was collected and calibrated using a silicon photodiode (S1137-1010BQ, Bunkoukeiki).

Electrochemical Impedance Spectroscopy (EIS). The impedance spectra of the solar cells were measured using an impedance gain-phase analyzer (Solartron Analytical 1260A) in the dark under inert atmosphere. The measurements were performed with a 50-mV ac sinusoidal signal and a 0.8-V dc bias potential. The frequency was swept from 1 MHz to 10 Hz. All fitting parameters and errors were analyzed using ZView software. The fitting parameters were R_c = contact resistance, C_{geo} = geometric capacitance of the OPV device, R_t = transport resistance, R_{rec} = recombination resistance, and a constant phase element (CPE). The equivalent capacitance (C_{eq}) of the CPE is given as[5,6]

$$C_{\mathrm{eq}} = \frac{\tau_{\mathrm{avg}}}{R_{\mathrm{rec}}} = \frac{(R_{\mathrm{rec}}Q)^{1/n}}{R_{\mathrm{rec}}} \tag{S3}$$

where τ_{avg} = average relaxation time, Q = the magnitude of the CPE, and n = ideality factor.

Space Charge Limited Current (SCLC) Mobility Measurements. The overall hole mobilities of the solar cells were calculated by fitting the dark current for hole-only diodes to the SCLC model. Hole-only devices were fabricated by substituting BCP/Al with MoO_3 (10 nm)/Au (100 nm). The fitting model is based on the Murgatroyd expression[7,8]

$$J(V) = \frac{9}{8}\varepsilon_0\varepsilon_r\mu_0 \exp\left(0.89\beta\sqrt{\frac{V-V_{\mathrm{bi}}}{L}}\right)\frac{(V-V_{\mathrm{bi}})^2}{L^3} \tag{S4}$$

where ε_0 = vacuum permittivity, ε_r = relative dielectric constant (3.3 for the organic layer), μ_0 = zero-field mobility, β = field activation factor, V_{bi} = built-in voltage, and L = thickness of the active layer.

References

(1) Wechwithayakhlung, C.; Packwood, D. M.; Chaopaknam, J.; Worakajit, P.; Ittisanronnachai, S.; Chanlek, N.; Promarak, V.; Kongpatpanich, K.; Harding, D. J.; Pattanasattayavong, P. Tin(II) Thiocyanate $Sn(NCS)_2$ – a Wide Band Gap Coordination Polymer Semiconductor with a 2D Structure. *J. Mater. Chem. C* **2019**, *7*, 3452–3462.

(2) Oliveira, F. S.; Cipriano, R. B.; da Silva, F. T.; Romão, E. C.; dos Santos, C. A. M. Simple Analytical Method for Determining Electrical Resistivity and Sheet Resistance Using the van Der Pauw Procedure. *Sci. Rep.* **2020**, *10*, 16379.

(3) Nečas, D.; Klapetek, P. Gwyddion: An Open-Source Software for SPM Data Analysis. *Cent. Eur. J. Phys.* **2012**, *10*, 181–188.

(4) Saeki, A.; Koizumi, Y.; Aida, T.; Seki, S. Comprehensive Approach to Intrinsic Charge Carrier Mobility in Conjugated Organic Molecules, Macromolecules, and Supramolecular Architectures. *Acc. Chem. Res.* **2012**, *45*, 1193–1202.

(5) Leever, B. J.; Bailey, C. A.; Marks, T. J.; Hersam, M. C.; Durstock, M. F. In Situ Characterization of Lifetime and Morphology in Operating Bulk Heterojunction Organic Photovoltaic Devices by Impedance Spectroscopy. *Adv. Energy Mater.* **2012**, *2*, 120–128.

(6) Guerrero, A.; Ripolles-Sanchis, T.; Boix, P. P.; Garcia-Belmonte, G. Series Resistance in Organic Bulk-Heterojunction Solar Devices: Modulating Carrier Transport with Fullerene Electron Traps. *Org. Electron.* **2012**, *13*, 2326–2332.

(7) Murgatroyd, P. N. Theory of Space-Charge-Limited Current Enhanced by Frenkel Effect. *J. Phys. D. Appl. Phys.* **1970**, *3*, 308.

(8) Liang, R.-Z.; Babics, M.; Seitkhan, A.; Wang, K.; Geraghty, P. B.; Lopatin, S.; Cruciani, F.; Firdaus, Y.; Caporuscio, M.; Jones, D. J.; Beaujuge, P. M. Additive-Morphology Interplay and Loss Channels in “All-Small-Molecule” Bulk-Heterojunction (BHJ) Solar Cells with the Nonfullerene Acceptor IDTTBM. *Adv. Funct. Mater.* **2018**, *28*, 1705464.

Table S1. Concentration of $Sn(SCN)_2$ in PEDOT:PSS solution, pH of mixed solution, PEDOT/PSS ratio from XPS S *2*p spectra, and measured optical band gap.

$Sn(SCN)_2$ starting concentration [mg mL^{-1}]	$Sn(SCN)_2$ volume [µL]	PEDOT:PSS volume [µL]	Additive concentration [% w/v]	pH of mixed solution	PEDOT/PSS ratio (from XPS S 2p peaks)	Optical band gap [±0.02 eV]
-	-	400	-	1.90	0.134	3.12
0 (Neat 1-propanol)	20	380	-	3.11	0.138	3.11
10	20	380	0.05	3.74	0.141	3.16
20	20	380	0.10	4.29	0.147	3.17
30	20	380	0.15	4.52	0.163	3.17
40	20	380	0.20	4.67	0.182	3.18

Table S2. Solar cell parameters employing PEDOT:PSS HTLs treated with varying concentrations of $Sn(SCN)_2$. The device area was 0.0707 cm^2. For each device parameters, the maximum (Max) or minimum (Min), average (Avg), and standard deviation (SD) values are given in this table.

HTL material	**J_{sc} [mA cm^{-2}]**			**V_{oc} [V]**			**FF [%]**			**PCE [%]**			**R_{sh} [Ω cm^2]**			**R_s [Ω cm^2]**			**No. of devices**
$Sn(SCN)_2$ added [% w/v]	*Max*	*Avg*	*SD*	*Max*	*Avg*	*SD*	*Max*	*Avg*	*SD*	*Max*	*Avg*	*SD*	*Max*	*Avg*	*SD*	*Min*	*Avg*	*SD*	
0.05	17.02	16.11	0.47	0.816	0.808	0.005	73.6	72.1	1.7	9.36	9.29	0.04	1168	865	159	0.6	1.2	0.3	10
0.10	17.00	16.40	0.41	0.817	0.810	0.004	74.4	72.3	1.5	9.51	9.41	0.05	1067	842	128	0.6	0.9	0.3	10
0.15	17.68	17.06	0.42	0.818	0.809	0.006	75.0	72.9	1.4	9.90	9.77	0.07	980	763	119	0.7	0.9	0.2	10
0.20	16.78	16.17	0.31	0.813	0.805	0.005	74.5	73.1	1.0	9.23	9.15	0.05	951	816	89	0.8	1.5	0.6	10
Pristine PEDOT:PSS	16.73	15.94	0.54	0.814	0.809	0.004	72.8	69.8	1.8	9.09	8.99	0.11	855	694	77	0.6	0.9	0.2	10

Table S3. Fitting parameters of solar cells analyzed from impedance spectroscopy under dark condition at a dc bias of 0.8 V. Numbers in the parentheses denote the fitting errors.

HTL material	**R_c [Ω]**	**R_t [Ω]**	**C_{geo} [nF]**	**R_{rec} [Ω]**	**Q [nF]**	***n***
Pristine PEDOT:PSS	16.85 (1.3%)	67.53 (1.2%)	12.0 (1.1%)	20.05 (3.9%)	30.3 (3.2%)	0.93 (0.3%)
0.15% w/v $Sn(SCN)_2$-treated PEDOT:PSS	14.51 (1.7%)	62.36 (1.5%)	13.3 (1.3%)	17.38 (4.5%)	34.1 (3.6%)	0.92 (0.3%)

Table S4. Hole mobility ($\mu_{h,SCLC}$) of hole-only devices extracted from the space-charge limited current (SCLC) analysis.

HTL material	**$\mu_{h,SCLC}$ [$\times 10^{-5}$ cm^2 V^{-1} s^{-1}]**	**Fitting error [$\times 10^{-5}$ cm^2 V^{-1} s^{-1}]**
Pristine PEDOT:PSS	3.67	0.40
0.15 w/v% $Sn(SCN)_2$-treated PEDOT:PSS	4.17	0.45

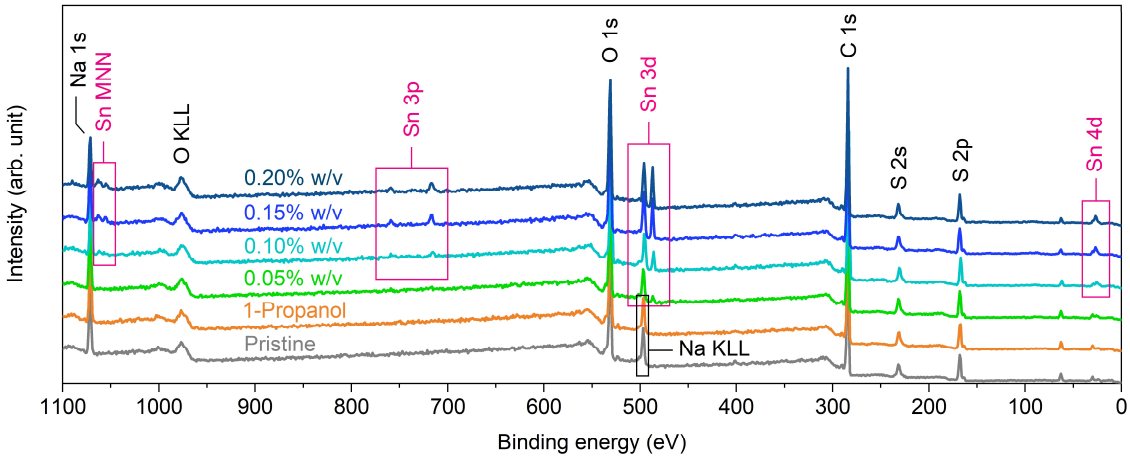

Figure S1. XPS survey scans.

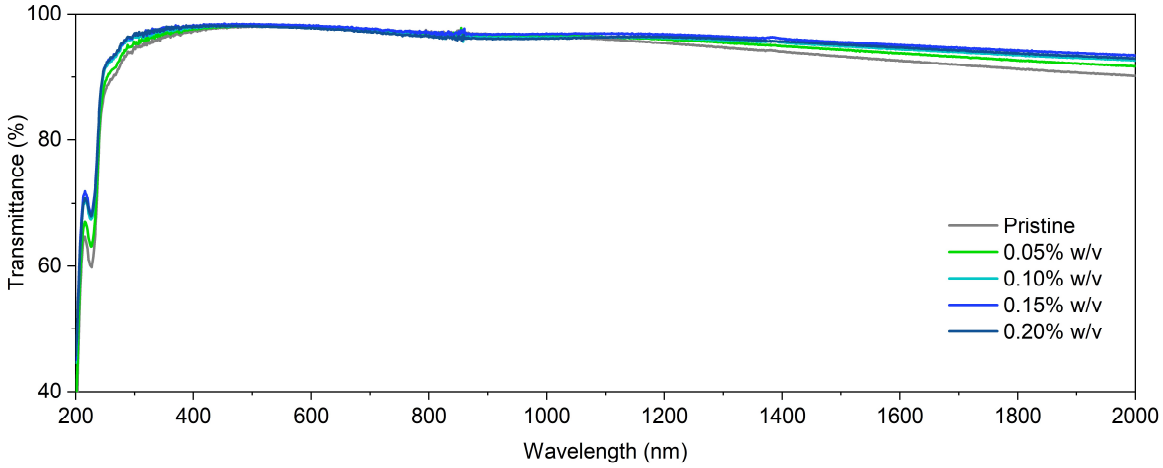

Figure S2. Full data range of UV-Vis-NIR transmission spectra.

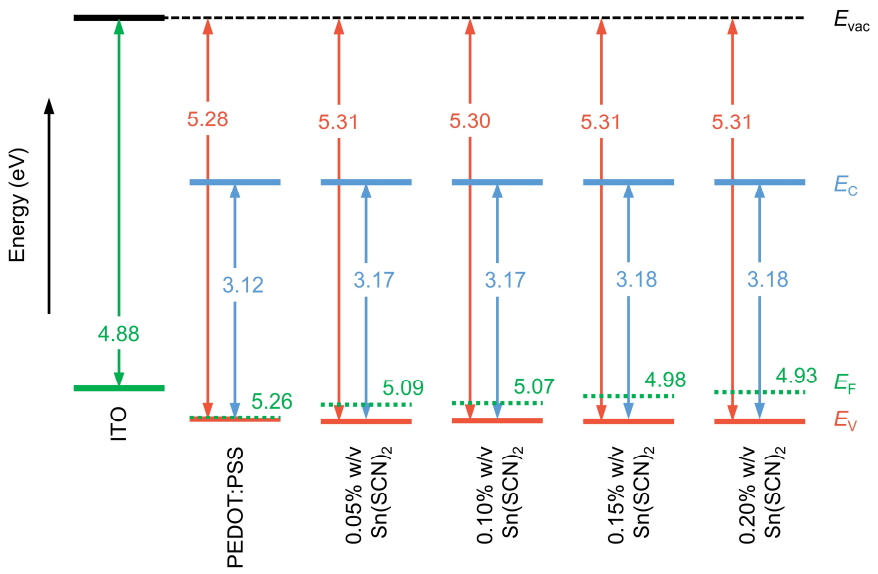

Figure S3. Schematic energy diagrams of the PEDOT:PSS layers added with different $Sn(SCN)_2$ concentrations, constructed using data from PYS, KP, and UV-Vis-NIR measurements. E_{vac} denotes the vacuum level, E_C the conduction band edge (solid blue lines), E_V the valence band edge (solid red lines), and E_F the Fermi level (dotted green lines).

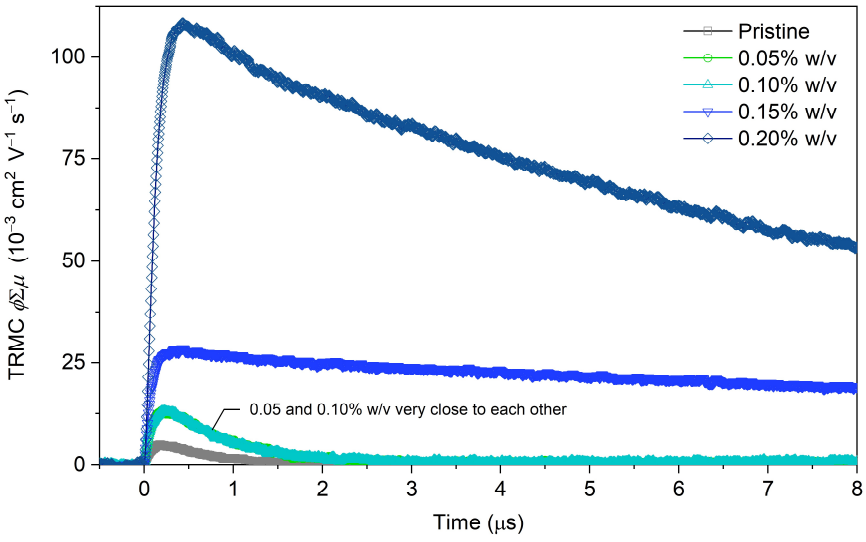

Figure S4. The product of charge carrier generation quantum efficiency and the sum of carrier mobilities ($\phi\Sigma\mu$) as a function of time measured by TRMC.

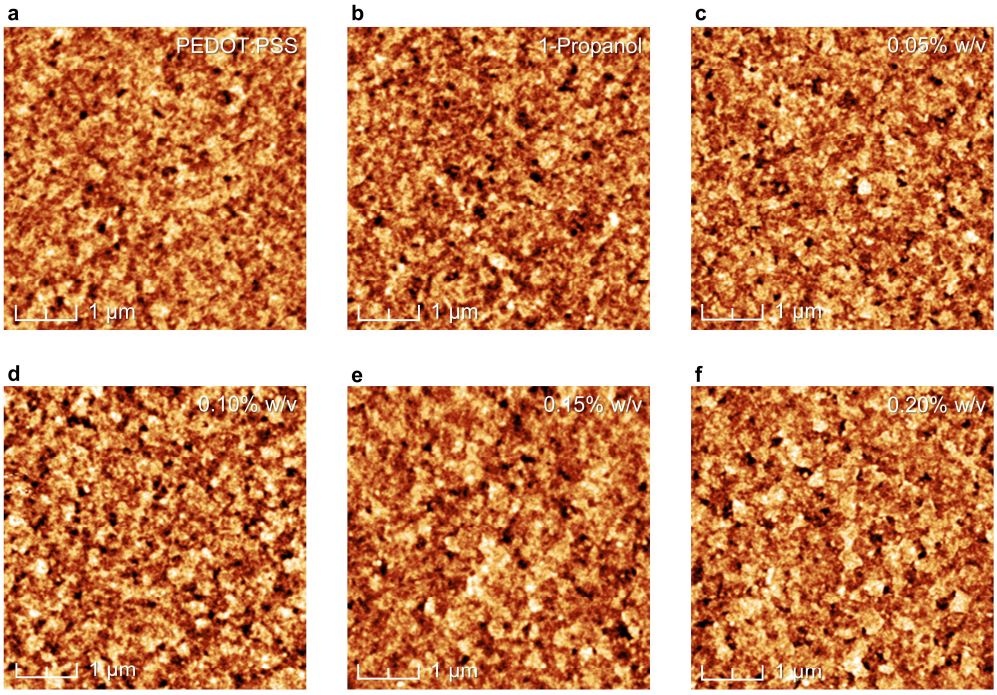

Figure S5. AFM topographic images over a 5×5 µm^2 area of: (a) pristine PEDOT:PSS, (b) PEDOT:PSS treated with neat 1-propanol, (c-f) PEDOT:PSS treated with 0.05, 0.10, 0.15, and 0.20% w/v of $Sn(SCN)_2$, respectively.

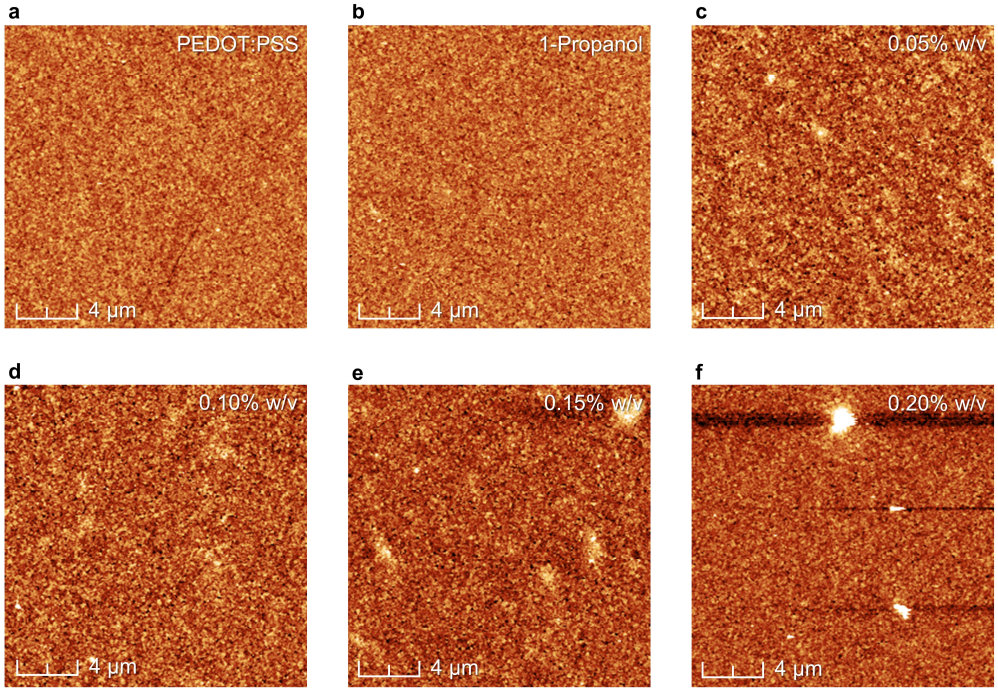

Figure S6. AFM topographic images over a 20×20 µm^2 area of: (a) pristine PEDOT:PSS, (b) PEDOT:PSS treated with neat 1-propanol, (c-f) PEDOT:PSS treated with 0.05, 0.10, 0.15, and 0.20% w/v of $Sn(SCN)_2$, respectively. The black streaks in (e) and (f) are artefacts due to the large particles.

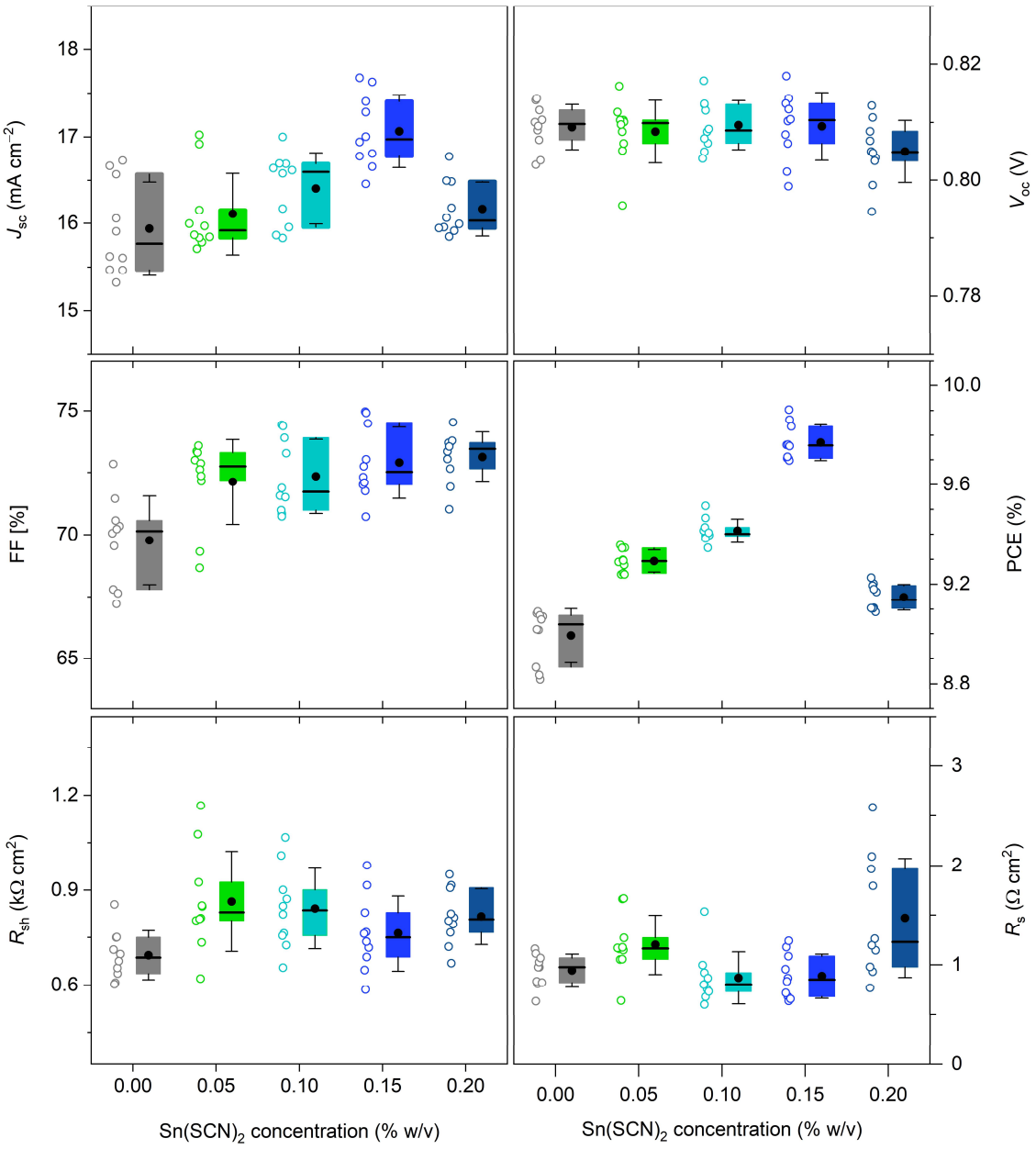

Figure S7. Scattered data points and box plots of OPV cell parameters for different concentrations of $Sn(SCN)_2$ as an additive in the PEDOT:PSS HTL. The boxes represent the 25th – 75th percentiles with the horizontal lines indicating the 50th percentiles. The black dots indicate the mean values, and the whiskers show the standard deviation.

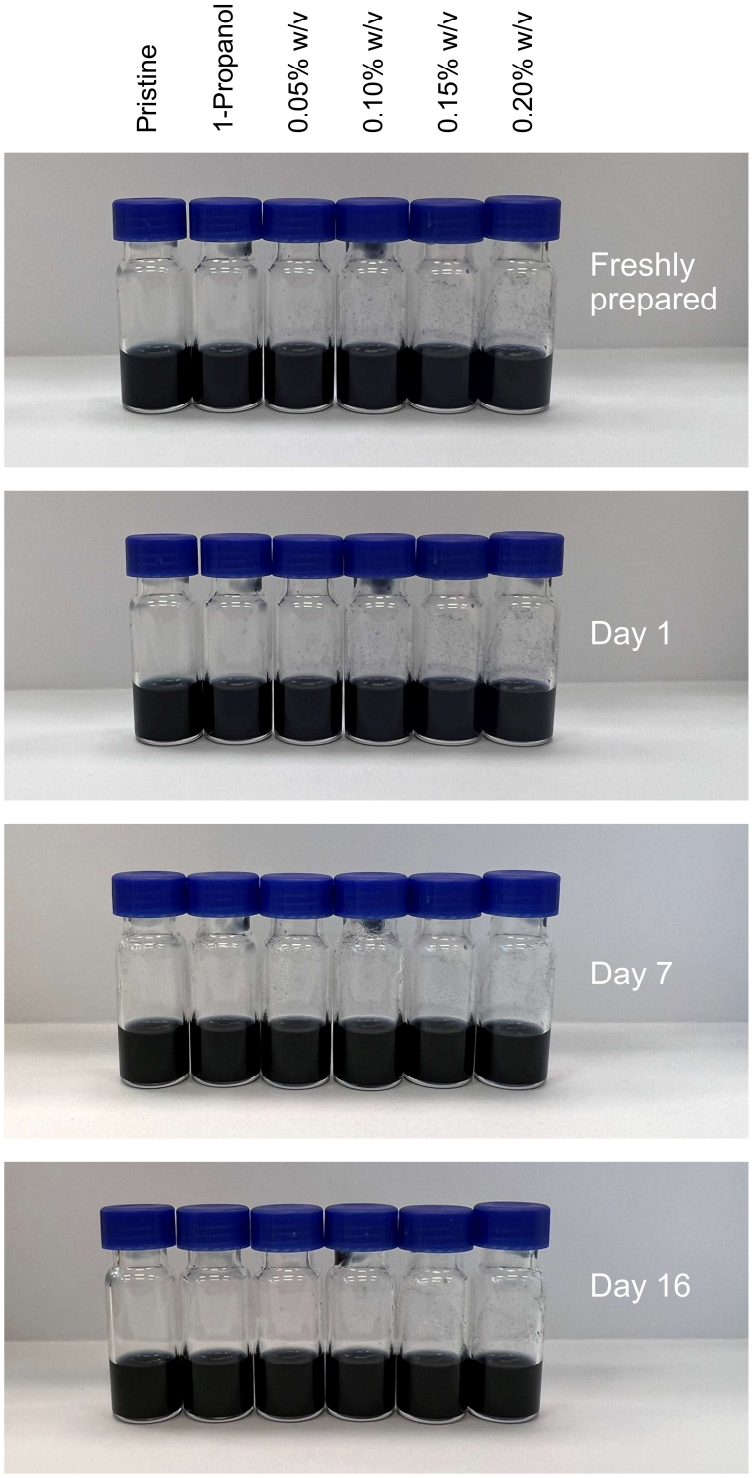

Figure S8. Images of the prepared solutions taken at different times.